High-z galaxies simulations: a benchmark for Global-MCAO

Elisa Portaluri[a,b], Valentina Viotto[a,b], Marco Gullieuszik[a,b], Davide Greggio[a,b,c], Maria Bergomi[a,b], Federico Biondi[a,b], Marco Dima[a,b], Jacopo Farinato[a,b], Demetrio Magrin[a,b], and Roberto Ragazzoni[a,b]

[a]Istituto Nazionale di Astrofisica - OAPD, vicolo dell'Osservatorio 5, Padova, Italy
[b]ADONI - Laboratorio Nazionale Ottiche Adattive - Italy
[c]Università degli Studi di Padova Dipartimento di Fisica e Astronomia G. Galilei, Vicolo dell'Osservatorio 3, Padova, Italy

ABSTRACT

Global-Multi Conjugate Adaptive Optics (GMCAO) can be a reliable approach for the new generation of Extremely Large Telescopes (ELTs) to address the issue of the sky coverage. It is based on the idea of using the largest possible technical field-of-view, to maximize the chance to find suitable reference stars. To prove that such innovative concept is robust and can be successfully used for studying faint objects, we build mock images of high-z galaxies and analyze them as if they were real and observed with an ELT that benefits of GMCAO. The results we obtained from the analysis of these images claim that this kind of method can be well used for extragalactic deep surveys, a key instrument that next generation telescopes will use to understand the origin and the evolution of galaxies.

Keywords: Global-MCAO, E-ELT, Galaxies: general, Galaxies: high-redshift

1. INTRODUCTION

The advent of powerful ELTs encouraged to explicate the new detailed observations with particularized theories and to elaborate numerical simulations for developing plausible interpretations. Their superb spatial resolution gives the possibility to study far objects and to puzzle over the complexities of one of the key questions of the extragalactic research in the last years: how galaxies formed and evolved. The paramount controversy is about which scenario is more eligible between a secular growth process,[1,2] in which large proto-galaxies formed early through a dissipational collapse, and the "hierarchical one",[3] in which galaxies are the result of successive mergers between small structures. The observations of the local Universe seem to converge in the mechanism of "downsizing",[4] where the galaxies evolution is linked to the mass: more massive systems form stars at high redshift ($z > 3$), while less massive ones take longer. Even if great progress has been done in tracing and modelling, understanding the formation and evolution of galaxies is a lively debated topic in astrophysics, it still defied a general accepted explanation.

Several astronomical surveys that investigate the galactic structures over a wide range of morphology were carried out and have revealed other important observational evidences, such as the evolution of the mean effective radius, R_e, for passive (i.e. early-type) galaxies,[5] the existence of a mean sequence for star-forming galaxies,[6] and color gradients in elliptical galaxies at high redshifts.[7] Moreover, despite of previsions, at high redshift very massive galaxies are already present, but they are smaller than nowadays ellipticals.[8–10] This suggests that they can not be the direct precursors of local galaxies and interaction phenomena may play a fundamental role for their evolution.[11–13]

At this point, a direct chance to discriminate the more plausible formation scenario and to understand their evolution is to look for spheroids and discs at $z > 1$ and compare their characteristics with those of local galaxies: studying the photometric properties of galaxies at different ages gives us the chance of understanding their assembling history and can provide important insight into the evolutionary history of galaxies.

*elisa.portaluri@oapd.inaf.it

Adaptive Optics Systems V, edited by Enrico Marchetti, Laird M. Close, Jean-Pierre Véran, Proc. of SPIE Vol. 9909, 99095Y
 · doi: 10.1117/12.2232758

This kind of study needs an excellent level of detail, possible only with space telescopes or with the application of Adaptive Optics (AO) techniques for ELT ground-based telescopes. In this framework, a challenging problem for AO is the fact that deep surveys are done in fields which are selected for having no bright stars. Therefore in this work we support the innovative idea of a Global-MCAO (GMCAO) system, proposed by [14], that can be applied to the next generation ground-based telescopes which will gather tens times more light than the largest optical and near infrared telescopes operating today. This technique maximizes the chance to find suitable reference stars in a wide field of view, a fundamental issue for the forthcoming ELTs, and in this sense helps the development of extragalactic science with ground-based instrumentation, often frozen out because of the small sky coverage.

We simulate deep field observations with an ELT that makes use of the GMCAO technique for correcting the distorted wavefronts. We take the E-ELT specifications as a reference and use them to build mock images of a set of high-z galaxies where we performed the source detection analysis.

The sample selection is described in Section 2. while the galaxies simulations are explained in Section 3. The results of the analysis and the conclusions are discussed in Section 4.

2. SAMPLE SELECTION

To simulate a deep field observation, we considered galaxies with a mass range of $\log M/M_{\odot} = 9, 9.3, 9.7, 10, 10.3$ observed at 6 different redshifts ($z = 0.25, 0.75, 1.25, 1.75, 2.25, 2.75$), following the results of [5] who studied the relationship between the structural parameters (size, as defined by the effective radius, $R_{\rm e}$, luminosity, as measured from total H-band magnitude, H, and total mass M) for 30000 galaxies from CANDELS HST survey. From the mass-size and the mass-luminosity relations, which are different for early- and late-type galaxies, we extrapolated our input parameters, graphically shown in Figure 1, and assumed a color of $H - K = 1$ mag. We used the concordance cosmology established by Planck,[15] with $H_0 = 67.8$, $\Omega_{\rm m} = 0.308$, for a flat Universe. With this assumptions, we built 60 galaxies which will represent our sample, as shown in Figure 2 for the best case (SR=30%) and for the median case (SR=17%), as discussed in the next session.

3. GALAXIES SIMULATOR

We built an image by adding simple models of astronomical objects, *i.e.* stars and galaxies, as specified in an input list, with our own IDL code. We took into account the effects of pixel scale, pixel sampling, background contribution, gain, readout noise, and exposure time. Noise consists of Poisson components. A typical near-IR sky background is the one measured at Cerro Paranal and included the contribution of thermal emission in the near-IR-bands. Specifically we adopted a total background of 12.8 mag arcsec^{-2} in the K band, as used in [16]. The galaxies were randomly distributed in a field-of-view of 50 × 50 arcsec and a pixel scale of 0.003 arcsec px^{-1} was chosen, to match the resolution of *Multi-AO Imaging Camera for Deep Observations* (MICADO[17]), that will be mounted on E-ELT. We used a Gain equal to 1 and simulated an exposure time of 3600 seconds. The profiles and templates are given elliptical shapes by specifying the scale radius for the major axis, $R_{\rm e}$, the ellipticity, $\epsilon = 1 - A/B$, where A/B is the minor axis to major axis axial ratio, the position angle, PA, defined counterclockwise from the x axis, and the coordinates of the centre, (x_0, y_0), of the object. They are mapped into 2-dimensional objects by an elliptical transformation that rotates and stretches them:

$$\begin{aligned} dx &= x - x_0 \\ dy &= y - y_0 \\ dX &= dx \times cos(PA) + dy \times sin(PA) \\ dY &= \frac{-dx \cdot \sin(PA) + dy \cdot \cos(PA)}{(A/B)} \\ r &= \sqrt{(dX^2 + dY^2)} \end{aligned} \tag{1}$$

where dx and dy are the object coordinates relative to the centre, dX and dY are the object coordinates in the transformed circular coordinates, and r is the circularly symmetric radius.

The objects are also characterized by the photometric laws that connotate their morphological types with a characteristic luminosity, I_0, *i.e.* the central value. We used simple flux profiles template, listed in Table 1.

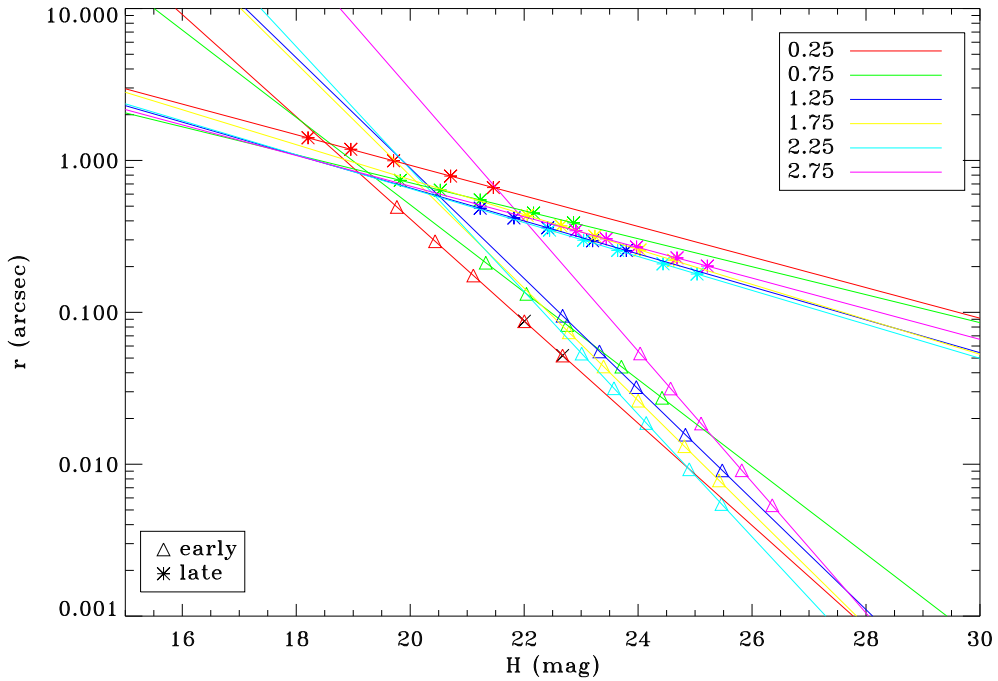

Figure 1. Input parameters for the simulated sample of galaxies in the deep field observation. Different colors are for different redshifts, as shown in the upper legend. The relationship between the axis parameters are taken from [5]. Triangles represent early-type galaxies, while asterisks are for late types. Solid lines represent the relationships between the structural parameters found by [5].

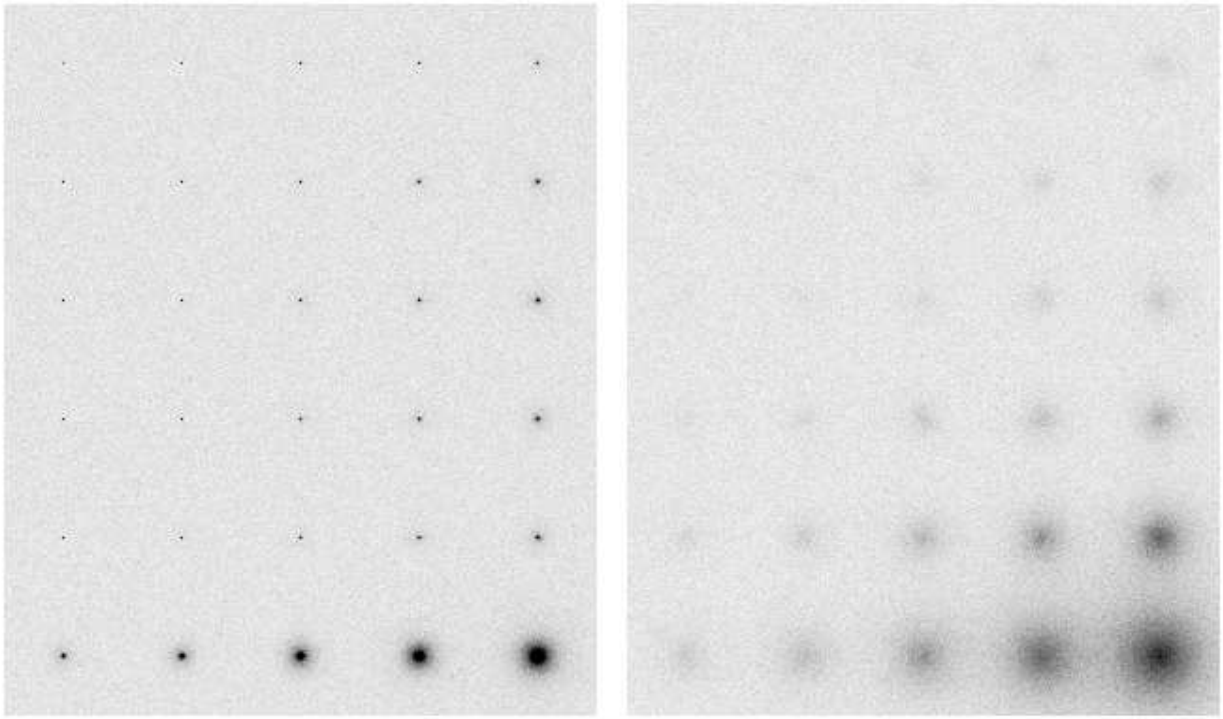

Figure 2. K-band images of the early- (left-hand panel) and late-type (right hand panel) sample galaxies in the 30% SR case. From left to right the mass increases (from $\log M/M_{\odot} = 9$ to $\log M/M_{\odot} = 10.3$), while from bottom to top the redshift becomes higher (from $z = 0.25$ to $z = 2.75$). The size for each image is 15×18 arcsec^2.

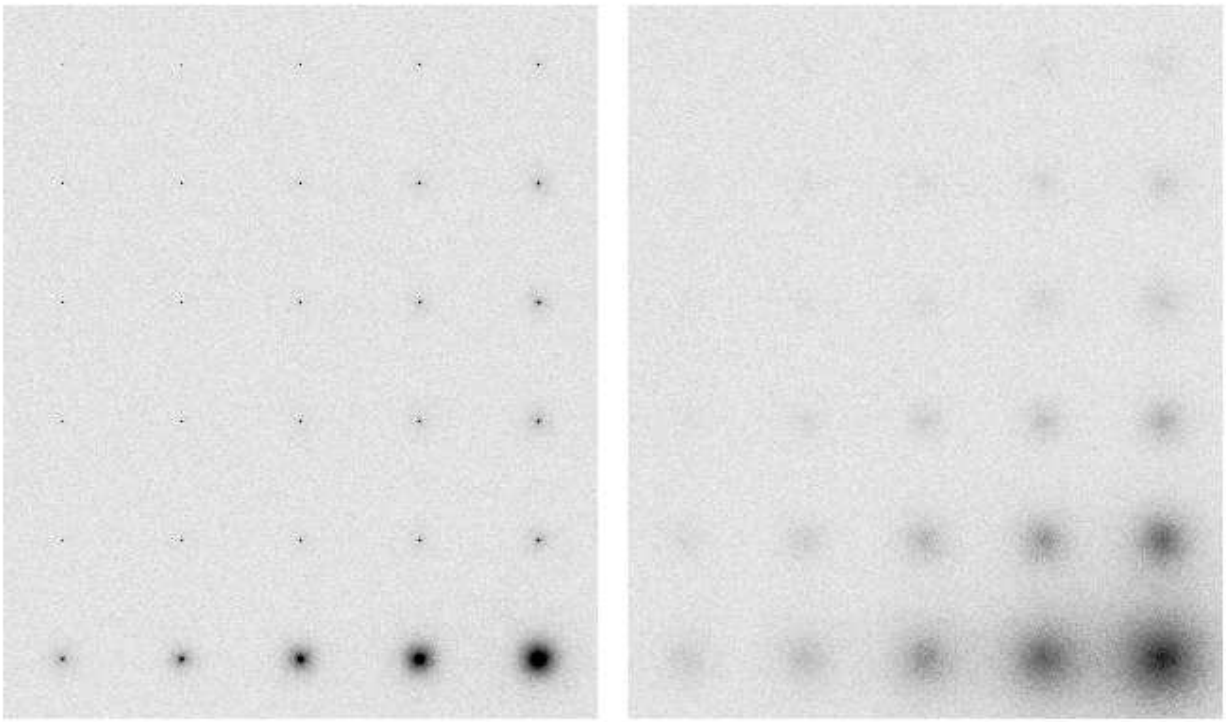

Figure 3. As for Figure 3, but the convolution is done with a PSF obtained with SR=17%.

Table 1. Photometric profiles for the galaxies simulation.

Model	Law	Param
Exponential	$I(r) = I_0 \cdot \exp(-1.6783 \cdot r/R_e)$	I_0, R_e
De Vaucouleurs	$I(r) = I_0 \cdot \exp(-7.67 \cdot (r/R_e)^{1/4} - 1)$	I_0, R_e

NOTES – Col.(1): Model name for the template object. Col.(2): Flux profile law for the corresponding model. Col.(3): Input parameter needed for building the object.

"Exponential" and "De Vaucouleurs" are two expressions of the Sérsic law[18] and represent common models for spiral and elliptical galaxies, respectively.[19,20]

As our main goal is to test the performance of a GMCAO-like system in detect faint galaxies, we did not take into account more complicated models or galactic substructures.

3.1 Image Convolution

The atmospheric turbulence above the telescope induces random phase distortions of the incoming wavefronts, resulting in optical aberrations in ground-based astronomical images.[21] For very small apertures, atmospheric turbulence has little effect on the image size, which is determined by the diameter of the telescope. Therefore for an ELT, it becomes a severe limitation for astronomers. AO is now commonly used to overcome this effect: a number of deformable mirrors, whose shape is continuously updated to match the current state of the atmospheric turbulence corrects the wavefronts in real time. Thanks to this technique, the energy concentration of the PSF almost reaches the resolution imposed by the diffraction limit, depending on instrumental characteristics. Within this framework, a good knowledge of the PSF of the system is mandatory for achieving an accurate image restoration. Its shape reflects how good is the system in compensating for the wavefront distortions, depending on both the structure of the object used as a reference (size, position and magnitude) and the local state of the turbulence, which continuously fluctuates.[22] As a result, the AO PSF is highly variable[23] with the time and across the field.

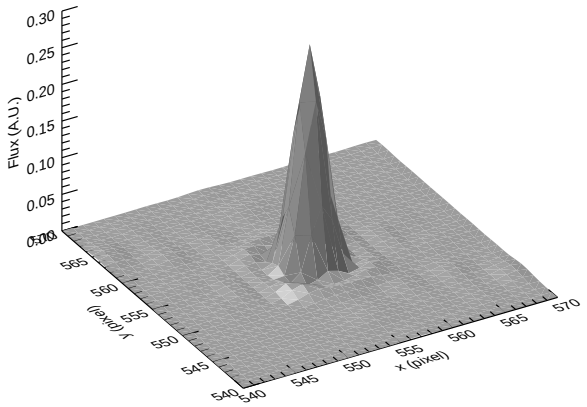

Figure 4. 3-dimensional PSF kernel obtained from corrected wavefronts matrix (ψ), in the 30% SR case.

Typically the long exposure PSF (at least in K band) of a ground telescope looks like a 2-dimensional Moffat function having the Full Width Half Maximum (FWHM) equal to the seeing. However, an AO PSF is completely different, because its shape is corrected by the deformable mirrors. The correction is only partial because the mirrors have a finite number of actuators behind their surface: they can use only a finite number of Zernike polinomials to fit the wavefronts. The resulting complex shape can no longer be easily represented with a unique analytical model and usually the common construction is with a narrow Moffat core to represent the diffraction limited core (width $\approx \lambda/D$), a broader Gaussian or Moffat halo for taking into account the contribution of the seeing (width $\approx \lambda/r_0$), and an external torus to estimate the fitting errors.[24]

We adopted an hybrid PSF, combining a residual map resulting from the simulated GMCAO-corrected wavefronts, and a Gaussian halo to simulate the external regions of the PSF. The PSF kernel, PSF_K, was obtained from a tomographic simulation code[25] that simulated an observation with an ELTs telescope in the region of the Chandra Deep Field South and used the stellar catalog USNO-B1.0 as references. The output wavefront matrix represents the residual map between the corrected wavefront and the flat (diffraction limited) one, as follows:

$$PSF_K = |\mathcal{F}[E]|^2 = \left|\mathcal{F}\left[\exp\left(\frac{-2\pi\imath\psi}{\lambda}\right)\right]\right|^2 \tag{2}$$

i.e. the square module of the Fourier Transform of the electric field, E. In our case λ is 2.1 μm, *i.e.* K band. ψs are 370×370 px^2 matrices, which we padded in order to obtain a spatial sampling of 0.003 arcsec px^{-1}. In fact the width of the Airy disc of this new matrix is $2\theta = 8$ px, where $\theta = 1.22\lambda/D = 1.22 \cdot 2.1 \times 10^{-6} \cdot 37 = 6.9243$ rad$= 0.0143$ arcsec. The pixel scale was $2\theta/8$=0.0036 arcsec px^{-1}, that we rescaled at 0.003 arcsec px^{-1} in order to match the future spatial resolution of the MICADO camera. We represented the external regions of the PSF as 2-dimensional Gaussian functions:

$$f(x,y) = A \cdot \exp\left[-\left(\frac{(x-x_0)^2}{2\sigma_x^2} + \frac{(y-y_0)^2}{2\sigma_y^2}\right)\right] \tag{3}$$

where A is the amplitude, x_0 and y_0 are the coordinates of the centre, $\sigma_x = \sigma_y = \sigma_{\mathrm{GAUSS}}$ is the standard deviation, linked to the seeing condition, especially with the Fried parameters, r_0:

$$\sigma_{\mathrm{GAUSS}} = \frac{seeing}{pxscale} = 1.22 \cdot \frac{\lambda/r_0}{pxscale} \tag{4}$$

We assumed r_0=0.75 m in K band, and we properly weighted the Gaussian contribution assessing the correct ratio between the peak of a diffraction-limited and the final PSF.

4. RESULTS AND CONCLUSIONS

We performed the source detection of all the images using SExtractor.[26] To have a robust analysis, we used a unique threshold for all the runs, *i.e.* 2σ level above the background. The statistics of whether the object was

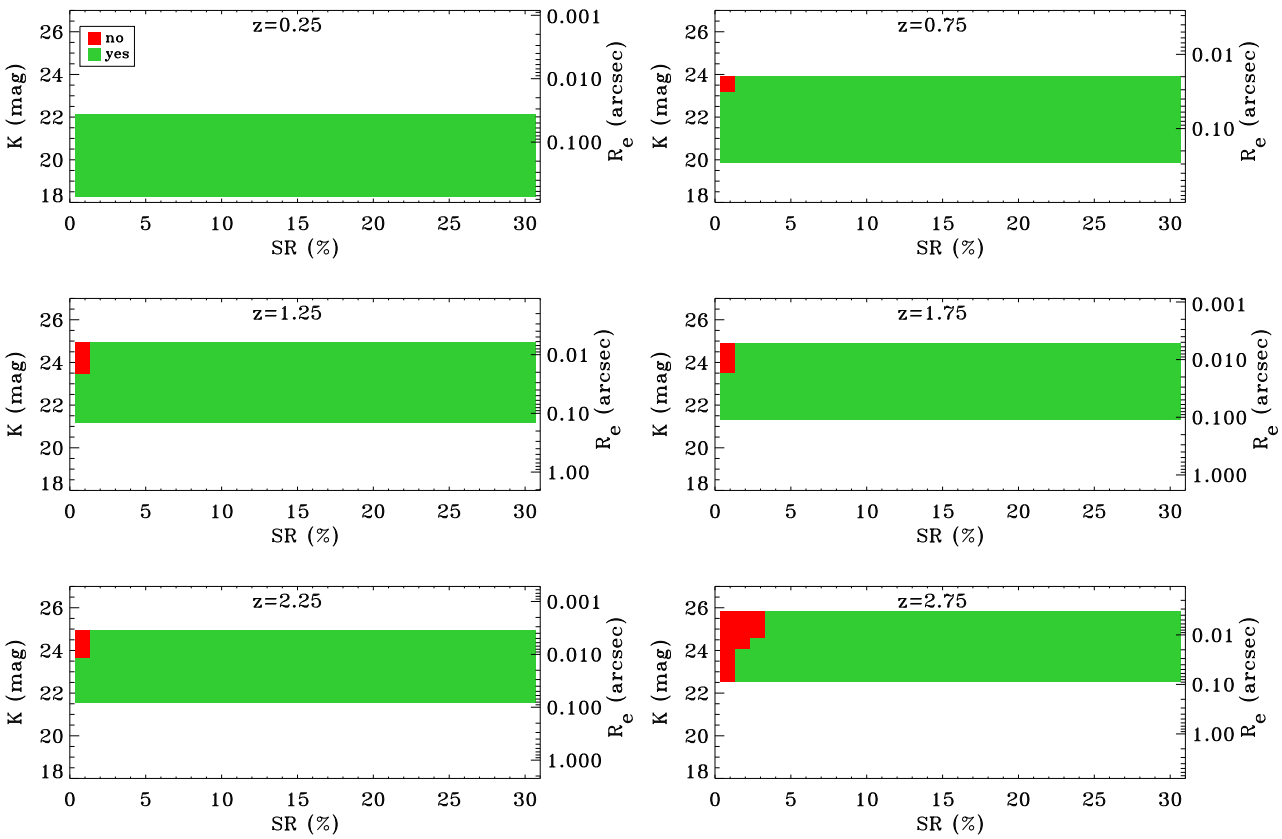

Figure 5. 2-dimensional map of objects detection as a function of the SR used to build the image and the K-band total magnitude. The analysis is shown for the early-type galaxies of the sample, for the 6 adopted redshifts. Green regions show where SExtractor has detected the object, while red regions are for missing detection.

or was not revealed as a function of the SR are shown Figure 5 and Figure 6. Green regions represent where the detection was successful, while red regions are for missing detection. We were able to easily detect the 98% and the 75% of early- and late-type galaxies of our sample, respectively. To increase the Signal-to-Noise ratio (S/N) of the images with the late-type objects, we performed a 2×2 binning and operated again the SExtractor estimation, increasing up to 87% the source detection, as shown by the yellow regions.

This analysis clearly shows that GMCAO would be able to recover early-type galaxies up to high redshifts even if the image has a low SR. This is very important especially because we have only few studies of elliptical small systems ($\log M/M_{\odot} < 10$). Because of late-type objects have a lower surface brightness distribution with respect to the early-type counterparts (*i.e.* galaxies that have the same total magnitude), we were able to easily detect spheroids at redshift up to 1.75 and we missed some detections of the very small systems at higher redshift. As expected, the detection improves as the SR become higher, and also when common techniques, as the image binning, are used to increase the S/N.

The mock GMCAO-based system we considered led to very interesting and robust results, especially if we take into account that the field we chose to examine is the Chandra Deep Field South. This region was selected because of the lack of bright (reference) stars, as usually done in the survey strategy. In this sense, our analysis shows how the GMCAO can overcome the limits of a MCAO system, and can give strong effort to the development of extragalactic science with ground-based instrumentation, often frozen out because of the small sky coverage.

In conclusion, to test the capability of GMCAO in a possible extragalactic deep survey operated with a next-generation telescope, we have studied a sample of 30 early and 30 late-type galaxies, assigned at 6 different

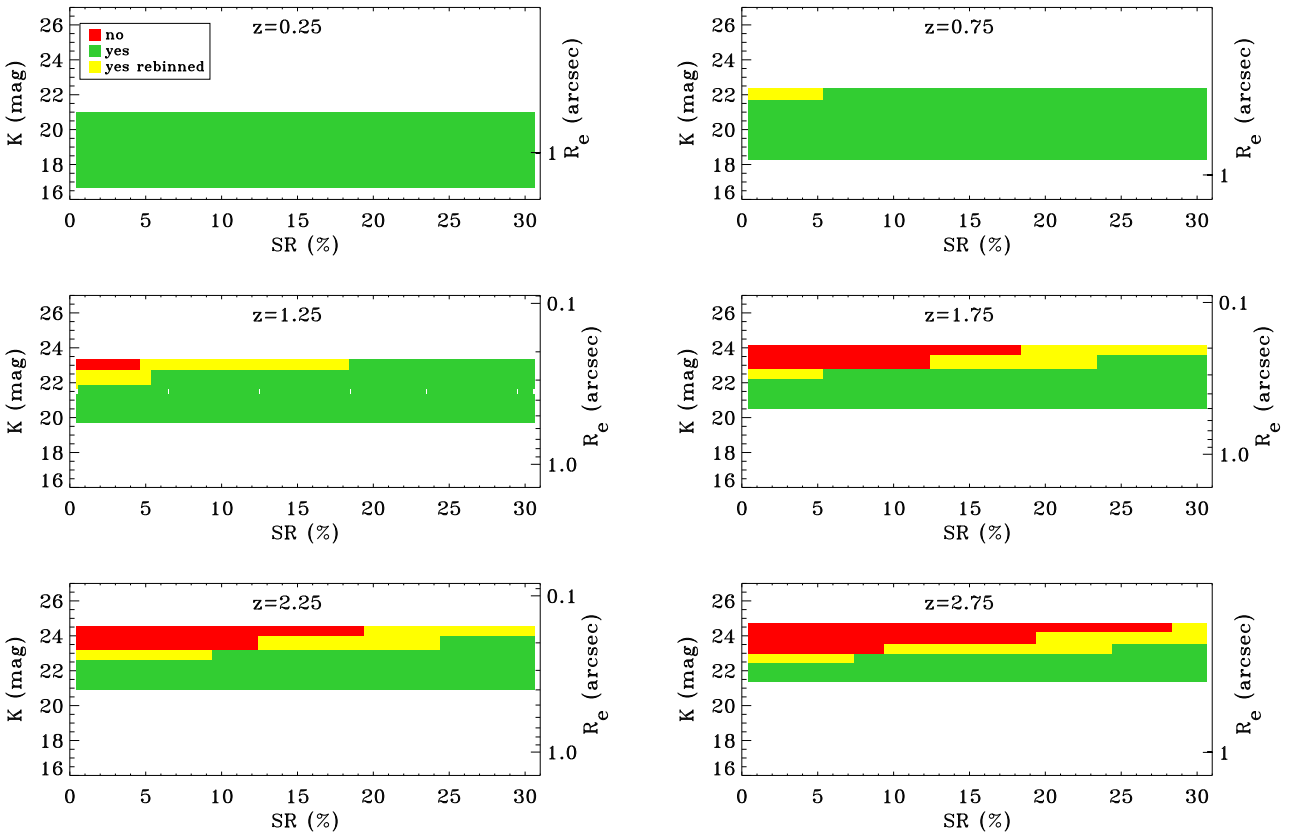

Figure 6. As for Figure 5, but for late-type galaxies of the sample. We have also performed a 2×2 binning, as explained in the text, to improve the S/N. This analysis increases significantly the detections, as clearly shown by yellow regions.

redshifts ($z = 0.25, 0.75, 1.25, 1.75, 2.25, 2.75$), and having physical properties (mass, size, luminosity) obtained following [5]. We have built mock images convolving the models with the PSF obtained simulating a E-ELT-like system that benefits of the GMCAO technique for correcting atmospheric distortions. We have analyzed them as if they were real, performing a source detection with common-used software.

The results obtained in this work represent a test case for GMCAO, which is a innovative concept that can address technical issues like the small sky coverage because it uses a very large technical field of view. We have demonstrated that it can represent a reliable approach to detect and study faint objects using the survey strategy, *i.e.* in star-poor regions. This kind of investigation is of great importance to study galaxies that can not be observed today because of they are too faint (the needs of bigger telescope to collect more light), low massive and too small (the needs of higher resolution). This will better address the questions linked to how galaxies formed and evolved, which is one of the key topics that are driving the development of the next generation of ELTs.

With this motivation, we will present in a forthcoming paper how GMCAO can be applied to carry out deep surveys, taking advantage of these preliminary results, but properly simulating a mock observation of the Chandra Deep Field South.

REFERENCES

[1] Eggen, O. J., Lynden-Bell, D., and Sandage, A. R., "Evidence from the motions of old stars that the Galaxy collapsed.," *ApJ* **136**, 748 (1962).

[2] Larson, R. B., "Dynamical models for the formation and evolution of spherical galaxies," *MNRAS* (1974).
[3] White, S. D. M., "Simulations of merging galaxies," *MNRAS* (1978).
[4] Cowie, L. L., Songaila, A., Hu, E. M., and Cohen, J. G., "New Insight on Galaxy Formation and Evolution From Keck Spectroscopy of the Hawaii Deep Fields," *AJ* (1996).
[5] van der Wel, A., Franx, M., van Dokkum, P. G., Skelton, R. E., Momcheva, I. G., Whitaker, K. E., Brammer, G. B., Bell, E. F., Rix, H.-W., Wuyts, S., Ferguson, H. C., Holden, B. P., Barro, G., Koekemoer, A. M., Chang, Y.-Y., McGrath, E. J., Häussler, B., Dekel, A., Behroozi, P., Fumagalli, M., Leja, J., Lundgren, B. F., Maseda, M. V., Nelson, E. J., Wake, D. A., Patel, S. G., Labbé, I., Faber, S. M., Grogin, N. A., and Kocevski, D. D., "3D-HST+CANDELS: The Evolution of the Galaxy Size-Mass Distribution since z = 3," *ApJ* (2014).
[6] Noeske, K. G., Weiner, B. J., Faber, S. M., Papovich, C., Koo, D. C., Somerville, R. S., Bundy, K., Conselice, C. J., Newman, J. A., Schiminovich, D., Le Floc'h, E., Coil, A. L., Rieke, G. H., Lotz, J. M., Primack, J. R., Barmby, P., Cooper, M. C., Davis, M., Ellis, R. S., Fazio, G. G., Guhathakurta, P., Huang, J., Kassin, S. A., Martin, D. C., Phillips, A. C., Rich, R. M., Small, T. A., Willmer, C. N. A., and Wilson, G., "Star Formation in AEGIS Field Galaxies since z=1.1: The Dominance of Gradually Declining Star Formation, and the Main Sequence of Star-forming Galaxies," *ApJ* (2007).
[7] Gargiulo, A., Saracco, P., Longhetti, M., La Barbera, F., and Tamburri, S., "Spatially resolved colours and stellar population properties in early-type galaxies at z ≈ 1.5," *MNRAS* (2012).
[8] Daddi, E., Dickinson, M., Chary, R., Pope, A., Morrison, G., Alexander, D. M., Bauer, F. E., Brandt, W. N., Giavalisco, M., Ferguson, H., Lee, K.-S., Lehmer, B. D., Papovich, C., and Renzini, A., "The Population of BzK-selected ULIRGs at z ˜ 2," *ApJ* (2005).
[9] van Dokkum, P. G., Franx, M., Kriek, M., Holden, B., Illingworth, G. D., Magee, D., Bouwens, R., Marchesini, D., Quadri, R., Rudnick, G., Taylor, E. N., and Toft, S., "Confirmation of the Remarkable Compactness of Massive Quiescent Galaxies at z ˜ 2.3: Early-Type Galaxies Did not Form in a Simple Monolithic Collapse," *ApJ* (2008).
[10] Cimatti, A., Cassata, P., Pozzetti, L., Kurk, J., Mignoli, M., Renzini, A., Daddi, E., Bolzonella, M., Brusa, M., Rodighiero, G., Dickinson, M., Franceschini, A., Zamorani, G., Berta, S., Rosati, P., and Halliday, C., "GMASS ultradeep spectroscopy of galaxies at z ≈ 2. II. Superdense passive galaxies: how did they form and evolve?," *A&A* (2008).
[11] Trujillo, I., Conselice, C. J., Bundy, K., Cooper, M. C., Eisenhardt, P., and Ellis, R. S., "Strong size evolution of the most massive galaxies since z ˜ 2," *MNRAS* (2007).
[12] Longhetti, M., Saracco, P., Severgnini, P., Della Ceca, R., Mannucci, F., Bender, R., Drory, N., Feulner, G., and Hopp, U., "The Kormendy relation of massive elliptical galaxies at z ˜ 1.5: evidence for size evolution," *MNRAS* (2007).
[13] Buitrago, F., Trujillo, I., Conselice, C. J., Bouwens, R. J., Dickinson, M., and Yan, H., "Size Evolution of the Most Massive Galaxies at 1.7 < z < 3 from GOODS NICMOS Survey Imaging," *ApJ* (2008).
[14] Ragazzoni, R., Arcidiacono, C., Dima, M., Dri, P., Farinato, J., Gentile, G., Magrin, D., and Viotto, V., "How to break the FoV versus thickness rule in MCAO," in [*Adaptative Optics for Extremely Large Telescopes*], 2003 (2010).
[15] Planck Collaboration, Ade, P. A. R., Aghanim, N., Arnaud, M., Ashdown, M., Aumont, J., Baccigalupi, C., Banday, A. J., Barreiro, R. B., Bartlett, J. G., and et al., "Planck 2015 results. XIII. Cosmological parameters," *ArXiv e-prints* (2015).
[16] Gullieuszik, M., Greggio, L., Falomo, R., Schreiber, L., and Uslenghi, M., "Probing the nuclear star cluster of galaxies with extremely large telescopes," *A&A* (2014).
[17] Davies, R., Ageorges, N., Barl, L., Bedin, L. R., Bender, R., Bernardi, P., Chapron, F., Clenet, Y., Deep, A., Deul, E., Drost, M., Eisenhauer, F., Falomo, R., Fiorentino, G., Förster Schreiber, N. M., Gendron, E., Genzel, R., Gratadour, D., Greggio, L., Grupp, F., Held, E., Herbst, T., Hess, H.-J., Hubert, Z., Jahnke, K., Kuijken, K., Lutz, D., Magrin, D., Muschielok, B., Navarro, R., Noyola, E., Paumard, T., Piotto, G., Ragazzoni, R., Renzini, A., Rousset, G., Rix, H.-W., Saglia, R., Tacconi, L., Thiel, M., Tolstoy, E., Trippe, S., Tromp, N., Valentijn, E. A., Verdoes Kleijn, G., and Wegner, M., "MICADO: the E-ELT adaptive optics imaging camera," in [*Ground-based and Airborne Instrumentation for Astronomy III*], *Proc. SPIE* **7735** (2010).

[18] Sérsic, J. L., [*Atlas de galaxias australes*], Cordoba, Argentina: Observatorio Astronomico, 1968 (1968).
[19] Freeman, K. C., "On the Disks of Spiral and so Galaxies," *ApJ* (1970).
[20] de Vaucouleurs, G., de Vaucouleurs, A., Corwin, Jr., H. G., Buta, R. J., Paturel, G., and Fouque, P., [*Third Reference Catalogue of Bright Galaxies*], Volume 1-3, XII, 2069 pp. 7 figs.. Springer-Verlag Berlin Heidelberg New York (1991).
[21] Roddier, F., "The effects of atmospheric turbulence in optical astronomy," *Progress in optics. Volume 19. Amsterdam, North-Holland Publishing Co., 1981, p. 281-376.* **19**, 281–376 (1981).
[22] Veran, J.-P., Rigaut, F., Maitre, H., and Rouan, D., "Estimation of the adaptive optics long-exposure point-spread function using control loop data.," *Journal of the Optical Society of America A* (1997).
[23] Tessier, E., "Analysis and calibration of natural guide star adaptive optics data," in [*European Southern Observatory Conference and Workshop Proceedings*], Cullum, M., ed., *European Southern Observatory Conference and Workshop Proceedings* **54**, 465 (1996).
[24] Schreiber, L., Diolaiti, E., Bellazzini, M., Ciliegi, P., Foppiani, I., Greggio, L., Lanzoni, B., and Lombini, M., "Handling a highly structured and spatially variable Point Spread Function in AO images," in [*Second International Conference on Adaptive Optics for Extremely Large Telescopes*], (2011).
[25] Viotto, V., Bergomi, M., Portaluri, E., Dima, M., Farinato, J., Greggio, D., Magrin, D., and Ragazzoni, R., "GMCAO for E-ELT: a feasibility study," in [*Adaptative Optics for Extremely Large Telescopes 4*], (2015).
[26] Bertin, E. and Arnouts, S., "SExtractor: Software for source extraction," *A&AS* (1996).